Journal of Structural Geology, Vol. 12, No. 7, pp. 835 to 850, 1990
Printed in Great Britain

0191-8141/90 $03.00+0.00

Episodic discrete and distributed deformation: consequences and controls in a thrust culmination from the central Pyrenees

NEIL T. GRANT*

Department of Earth Sciences, The University, Leeds LS2 9JT, U.K.

(*Received* 25 *August* 1989; *accepted in revised form* 23 *January* 1990)

Abstract—The Pic de Port Vieux culmination is a 0.5 km long thrust culmination in the footwall of the Gavarnie Thrust in the central Pyrenees. The culmination comprises a set of blind thrusts that imbricate a 50 m thick Mesozoic cover sequence, comprising Triassic red beds and Upper Cretaceous limestone, sandwiched between underlying Hercynian basement and the overlying Palaeozoic strata of the Gavarnie thrust sheet. An intense cleavage developed within the culmination associated with the oblique tip-lines of the thrusts as they climbed from the basement into the cover strata. Detailed mapping shows that the distributed strain associated with the fault tips locally re-activated earlier folded thrusts, creating upper detachments to the system, and produced a set of new overstepping isolated faults. The main detachment occurred along the roof of the culmination using the back-limbs of folds in the roof thrust. The movement on these detachments can be demonstrated to have been episodic, with periods of fault slip producing splays that were then folded during periods when distributed deformation was dominant. The main control on this episodic deformation is modelled as the result of feedback between increase in fluid pressure associated with inelastic porosity reduction during cleavage development, and fluid pressure bleed-off associated with fault zone dilatancy in the culmination.

INTRODUCTION

IN THE external portions of foreland fold-and-thrust belts, deformation is discrete and dominated by fault displacement and the flexural slip of stratal surfaces (Dahlstrom 1969). These combine to preserve near-plane strain deformation. In the more internal portions of thrust belts more distributed deformation mechanisms are activated due to higher temperatures and pressures. Here diffusive mass transfer and crystal-plasticity become important and compete with the discrete mechanisms to accommodate strain that need not necessarily be plane. The controls on which mechanisms dominate at any time are a function of both lithology and environmental conditions (e.g. Knipe 1989) and they may change both spatially, as thrusts cut across different stratal units and *P/T* gradients, and temporally, as a result of large strain and grain-size changes (e.g. Mitra 1982), for example, or as a result of fluid overpressuring (e.g. Cox & Etheridge 1989). The result is that strain accommodation mechanisms can be expected to change during deformation.

This paper documents a field example where episodic changes between discrete and distributed deformation mechanisms occurred during structural growth. The setting is a 0.5 km cross-strike section through a small thrust culmination in the central Pyrenees. This structure presents an opportunity to study some of the consequences of, and to assess the most likely controls, on this type of deformation switching. The aim is to demonstrate the types of structures produced and to relate these to both the mechanical stratigraphy and the environmental conditions during thrusting. In particular, the importance of high fluid pressures in influencing rock response to deformation will be emphasized.

GEOLOGICAL SETTING

The Pyrenees represent an Alpine orogenic belt that formed largely by thrust-related processes (Choukroune & Seguret 1973, Fischer 1984, Parish 1984, Deramond *et al.* 1985, Williams & Fischer 1985, Fontbote 1986, Seguret & Daignières 1986) during convergence between Iberia and Europe in the end-Cretaceous to late Eocene interval (Mattauer & Henry 1974). The belt is distinct from many other Alpine orogenic belts in that its structural evolution was not associated with syntectonic regional metamorphism or regionally developed penetrative deformation (Banda & Wickam 1986).

The belt comprises both external and internal thrust sheets. The former are exposed in the south where a syntectonic foreland basin (the South Pyrenean Tertiary Basin) was imbricated by a thin-skinned foreland-propagating thrust system (Labaume *et al.* 1985). The latter are exposed in the basement-cored centre of the belt and comprise two levels of thrust sheets (Muñoz *et al.* 1986): middle thrust sheets that thrust basement over cover, and lower thrust sheets that imbricate mid-crustal basement. The structure described in this paper occurs directly in the footwall of one of the middle thrust sheets: the Gavarnie Thrust in the central Pyrenees.

The Gavarnie Thrust places Upper Palaeozoic metasediments over a Mesozoic cover sequence that rests unconformably on Hercynian migmatitic basement thought to be Cambro-Ordovician in age (Van Lith 1965). The structure that is the focus of this paper is the Pic de Port Vieux culmination (Grant 1989), a small thrust culmination exposed in the footwall of the Gavar-

*Present address: Conoco (U.K.) Ltd, 129 Park Street, London W1, U.K.

nie thrust in Cirque de Barroude (Fig. 1a). This culmination is itself located near the crest of a regional culmination in Gavarnie thrust (Fig. 1b) that is thought to have formed as a result of the stacking of blind 'lower' thrusts within the basement (Parish 1984, Muñoz *et al.* 1986, Grant 1989).

LITHOSTRATIGRAPHY OF THE PIC DE PORT VIEUX CULMINATION

A cross-section through the culmination is shown in Fig. 2 and a schematic stratigraphic section through the structure is shown in Fig. 3. The culmination occurs within the thin layer of Mesozoic cover (Triassic red beds and Upper Cretaceous limestone) sandwiched between the Hercynian basement and the Gavarnie thrust sheet. The basement comprises folded migmatized psammites and quartz–biotite schists, both of which possess a layer-parallel schistosity. These are locally intruded by syntectonic net-vein complexes and post-tectonic granodiorite sills, dykes and pods. The folds have N–S and E–W trends corresponding to the regional Hercynian D_1 and D_2 episodes, respectively (Deramond *et al.* 1980). Petrographic work coupled with XRD and microprobe analyses has shown that the basement strata in the Cirque de Barroude have suffered advanced argillic alteration (Grant 1989) and have been converted into a quartz–pyrophyllite–phengite rock. This pervasive alteration is probably late Hercynian in age, as clasts of altered basement can be found in the overlying Triassic strata.

The Triassic red beds lie unconformably on the basement with a basal conglomerate layer infilling an undulatory erosion surface. Figure 4 is a structural–sedimentary log through the Triassic strata which comprises a predominantly mudstone sequence with thin interbedded fining-upwards sandstone units. These units are interpreted as the products of waning sheet floods or broad shallow channels that crossed a distal flood plain environment (Grant 1989). This interpretation agrees with those of Zwart (1979) and Lucas (1985) who consider the Triassic deposits in the central Pyrenees the products of a braided alluvial system.

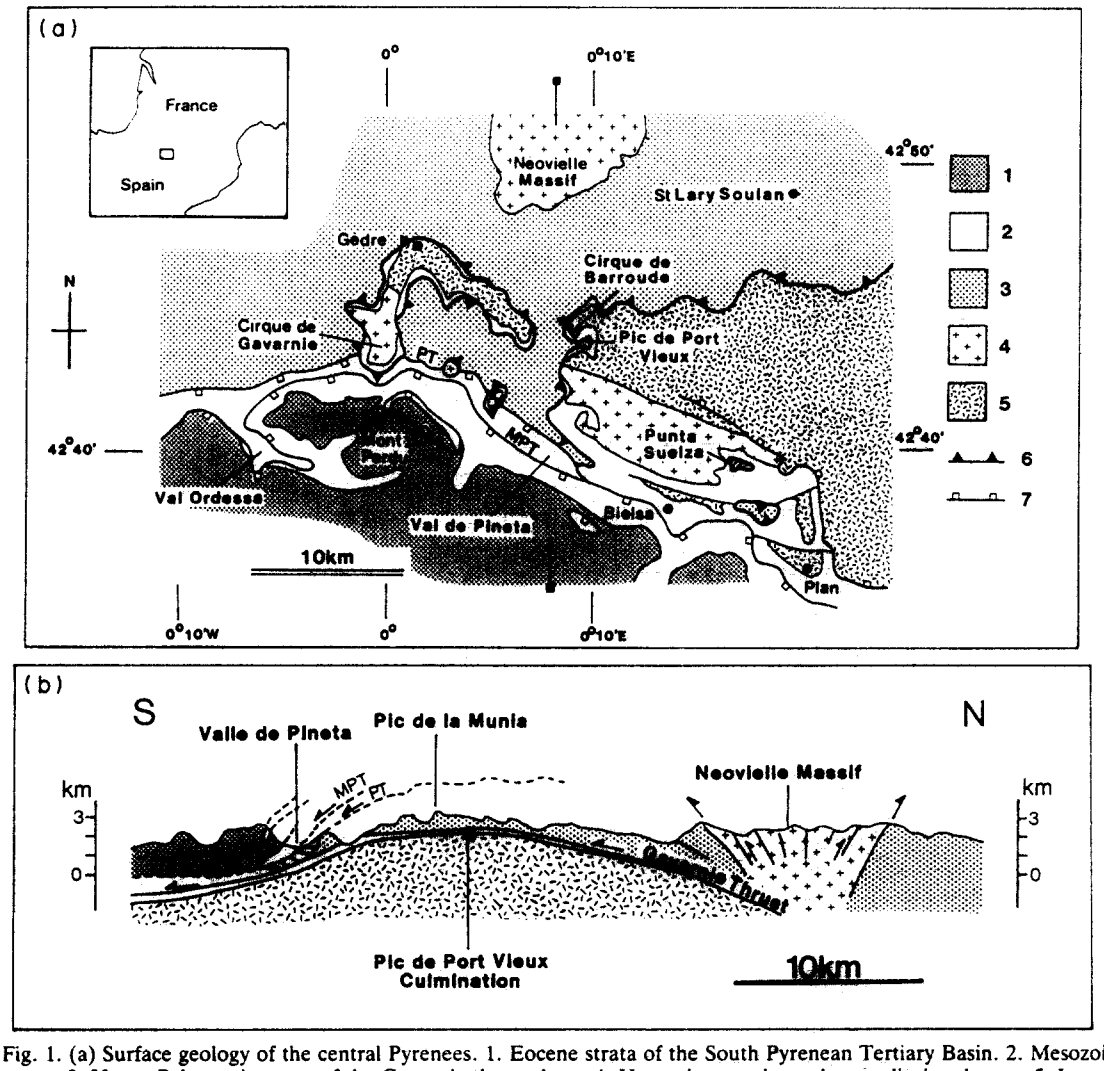

Fig. 1. (a) Surface geology of the central Pyrenees. 1. Eocene strata of the South Pyrenean Tertiary Basin. 2. Mesozoic strata. 3. Upper Palaeozoic strata of the Gavarnie thrust sheet. 4. Hercynian granite and granodiorite plutons. 5. Lower Palaeozoic Hercynian metasediments. (b) Section A–A′ showing location of the PPV culmination. The displacement on the Gavarnie Thrust in the plane of the section is approximately 11.5 km. The thrust is folded into a large culmination by blind thrusts in the basement (not shown).

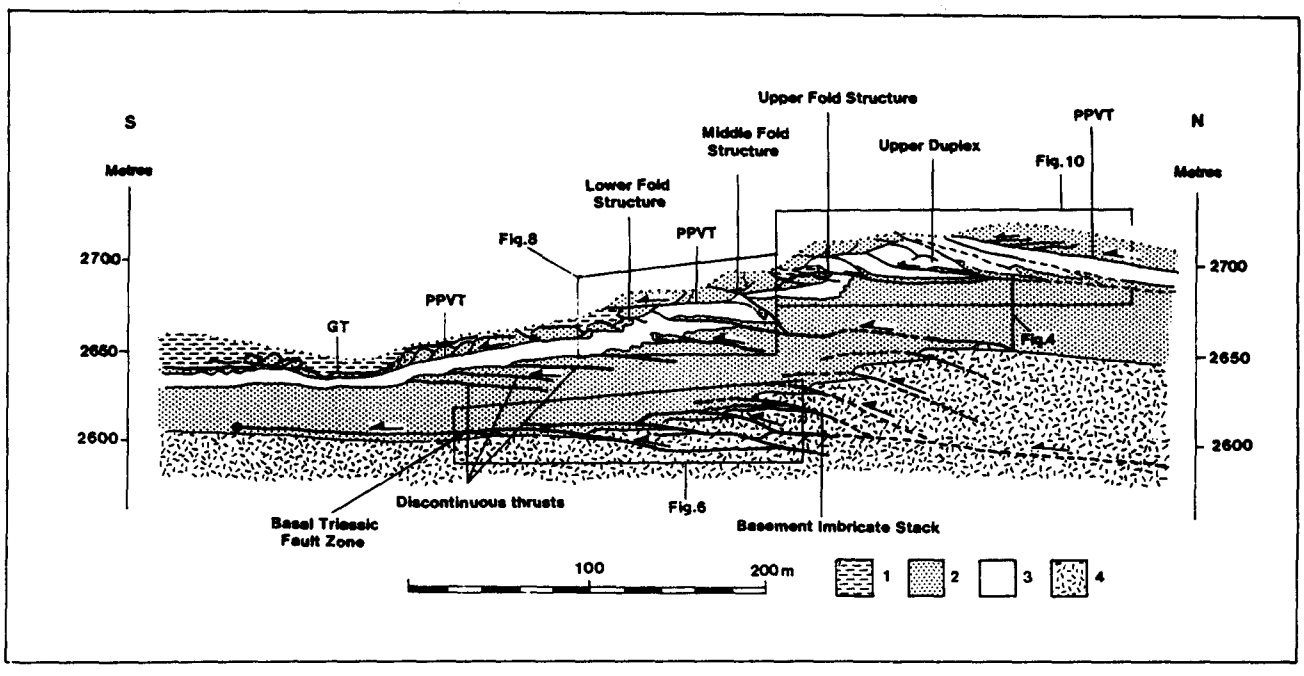

Fig. 2. N–S cross-section through the Pic de Port Vieux culmination. The main structures discussed in the text are named together with the relevant figures. 1. Silurian graphitic phyllite of the Gavarnie thrust sheet. 2. Triassic red beds. 3. Upper Cretaceous limestone. 4. Hercynian basement.

The Cretaceous limestone rests with planar unconformity on the Triassic red beds or directly on the basement. The limestone has been strongly deformed during movement on the Gavarnie Thrust and locally possesses a strongly mylonitic fabric. The predominantly biomicrite protolith is Cenomanian to Santonian in age (Martinez 1968).

On Pic de Port Vieux, the Cretaceous limestone is

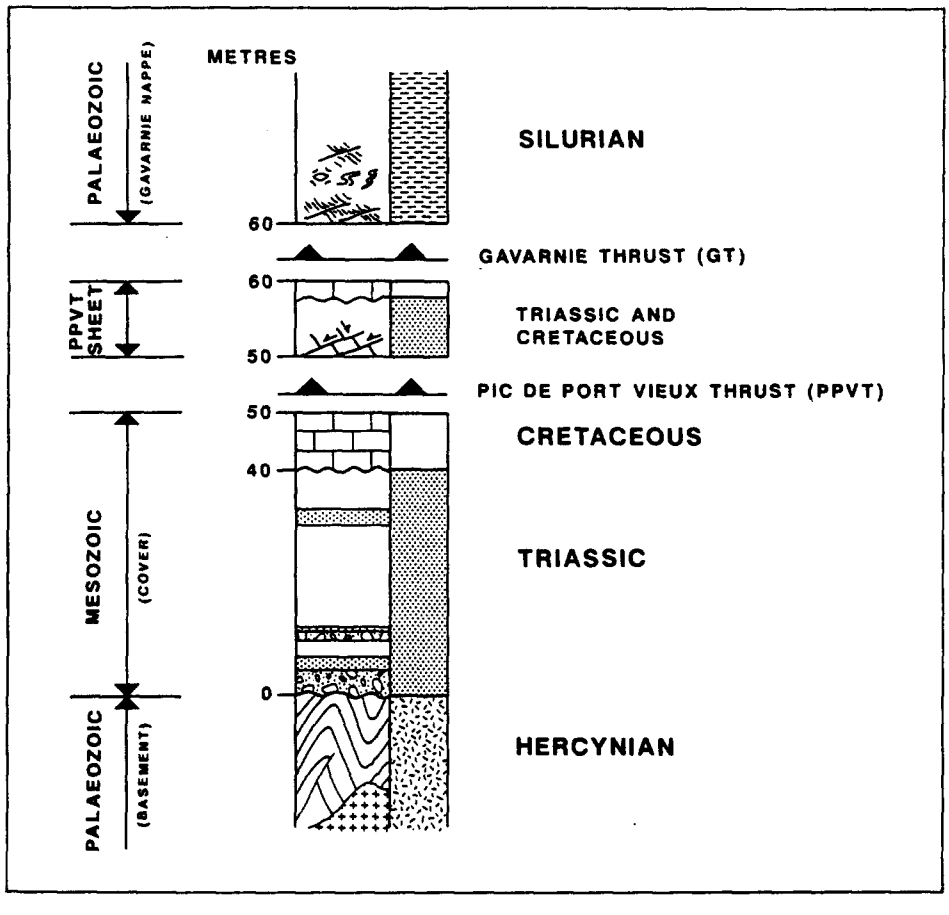

Fig. 3. Schematic stratigraphic log through the culmination.

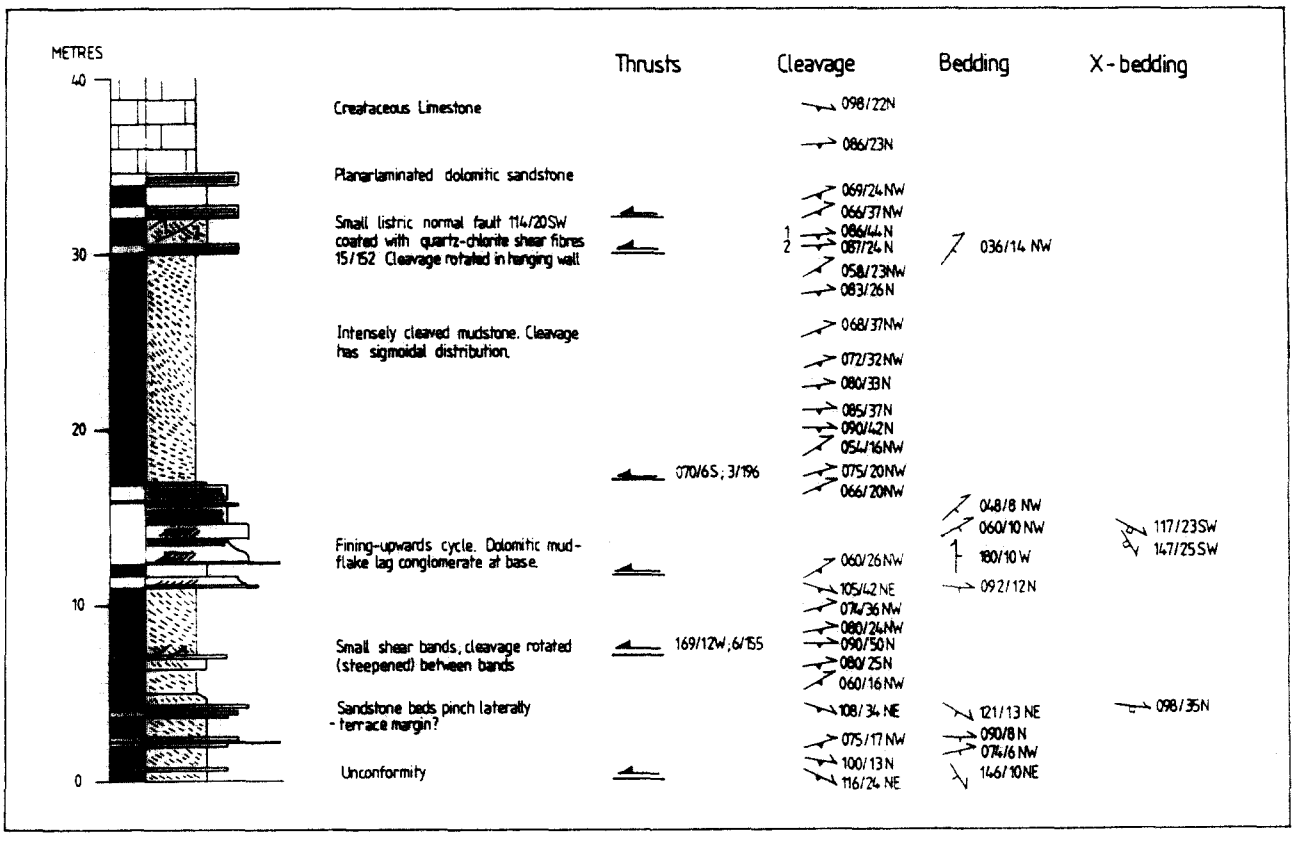

Fig. 4. Structural–sedimentological log through the Triassic strata of Pic de Port Vieux. The location of the log is shown in Fig. 2.

overlain first by the Pic de Port Vieux thrust sheet (Grant 1989) (a thin thrust sheet that duplicates the cover stratigraphy) and then by the Palaeozoic strata of the Gavarnie thrust sheet. The Gavarnie thrust sheet comprises intensely sheared Silurian graphitic phyllite possessing a strong slaty foliation that anastomoses around boudinaged quartz-vein augen or boulder-size pods of granite or dolomitic limestone. This phyllite is cut extensively by shear bands in a zone 30 m wide bordering the Gavarnie Thrust.

CONDITIONS OF DEFORMATION

The physical conditions during the deformation have been estimated from a microthermometric analysis of fluid inclusions in fault-related vein quartz (Grant 1989, Grant *et al.* in press). Fluid inclusion trapping appears to have occurred in a temperature range of 250–300°C with a fluid pressure of between 1.5 and 2.0 kb. There is evidence to suggest that the fluid pressure was near lithostatic during the faulting (see later) and these conditions are therefore believed to approximate the conditions under which deformation occurred. The stability of pyrophyllite–phengite intergrowths in the altered Hercynian basement, the absence of dislocation-creep textures and predominance of fracturing or dislocation-glide textures in deformed quartz grains in the fault zones are compatible with these conditions.

THE STRUCTURE OF THE PIC DE PORT VIEUX CULMINATION

The Pic de Port Vieux Culmination (PPV culmination) comprises the upper 100 m of Pic de Port Vieux. It was produced by a number of thrusts located both within the Hercynian basement and within the Mesozoic cover (Fig. 2). It occupies a similar structural position to the Lower and Upper Troumouse duplexes exposed further west in the Gavarnie window (Parish 1984) but is a separate structure (Grant 1989). The Pic de Port Vieux Thrust (PPVT) forms the roof thrust to the culmination and has a minimum displacement of 0.85 km. Two main structures occur below the PPVT: the Basement Imbricate Stack (BIS) and the Upper Duplex (Fig. 2). The former is a set of thrusts that imbricate the Hercynian basement and basal Triassic strata, the latter a small duplex that shortens the Cretaceous limestone beneath the summit of the mountain. Cumulative displacement in both structures is of the order or 60–70 m based on bedding offsets. These two structures are separated by 30–40 m of cleaved and folded Triassic and Cretaceous strata that are cut by discontinuous thrusts. These faults tend to form tip folds within the Cretaceous limestone that fold the overlying PPVT sheet. Three main folds are present and are referred to as the Upper, Middle and Lower Fold Structures (Fig. 2).

Three locally developed phases of thrusting have been identified within the culmination and can be related to a progressive deformation sequence. The PPVT and

Gavarnie Thrust (GT) are considered for the purposes of this description as phase 2 thrusts. The Basement Imbricate Stack, Upper Duplex and discontinuous thrusts that fold the PPVT sheet are together classified as phase 3 structures. A model summarizing the deformation sequence in the culmination is shown in Fig. 5.

Phase 1 *thrusts* (*P*1)

The first phase thrusts occur as small isolated structures that duplicate the Triassic and Cretaceous strata below the PPVT (Fig. 2). They belong to a separate thrust phase as they are truncated (breached) by both the GT and the PPVT. The relatively small P1 thrusts appear to represent localized structures that branched from a décollement within the Triassic strata possibly along or adjacent to the irregular basal unconformity. They have displacements of between 10 and 30 m where they intersect the Cretaceous unconformity. These thrusts represent "upper thrusts" in the classification of Muñoz *et al.* (1986).

Phase 2 *thrusts* (*P*2)

The second phase of thrusting within the culmination is represented by the emplacement of the GT and PPVT. These faults intersect the earlier P1 thrusts as they climb gently across the Cretaceous limestone and are therefore out-of-sequence (Morley 1987). The displacement on the GT is estimated as a minimum of 11.5 km (Fig. 1b) in the plane of section (Grant 1989). Both the GT and PPVT moved north-to-south, indicated by mylonite stretching lineations and quartz mineral-fibre lineations along the fault planes. Emplacement of the thrusts produced a mylonite foliation in the Cretaceous limestone and a slaty cleavage in the Triassic red beds (see Fig. 4). The Triassic fabric terminates downwards along the basal unconformity or along a fault that follows the top of the basal conglomerate unit.

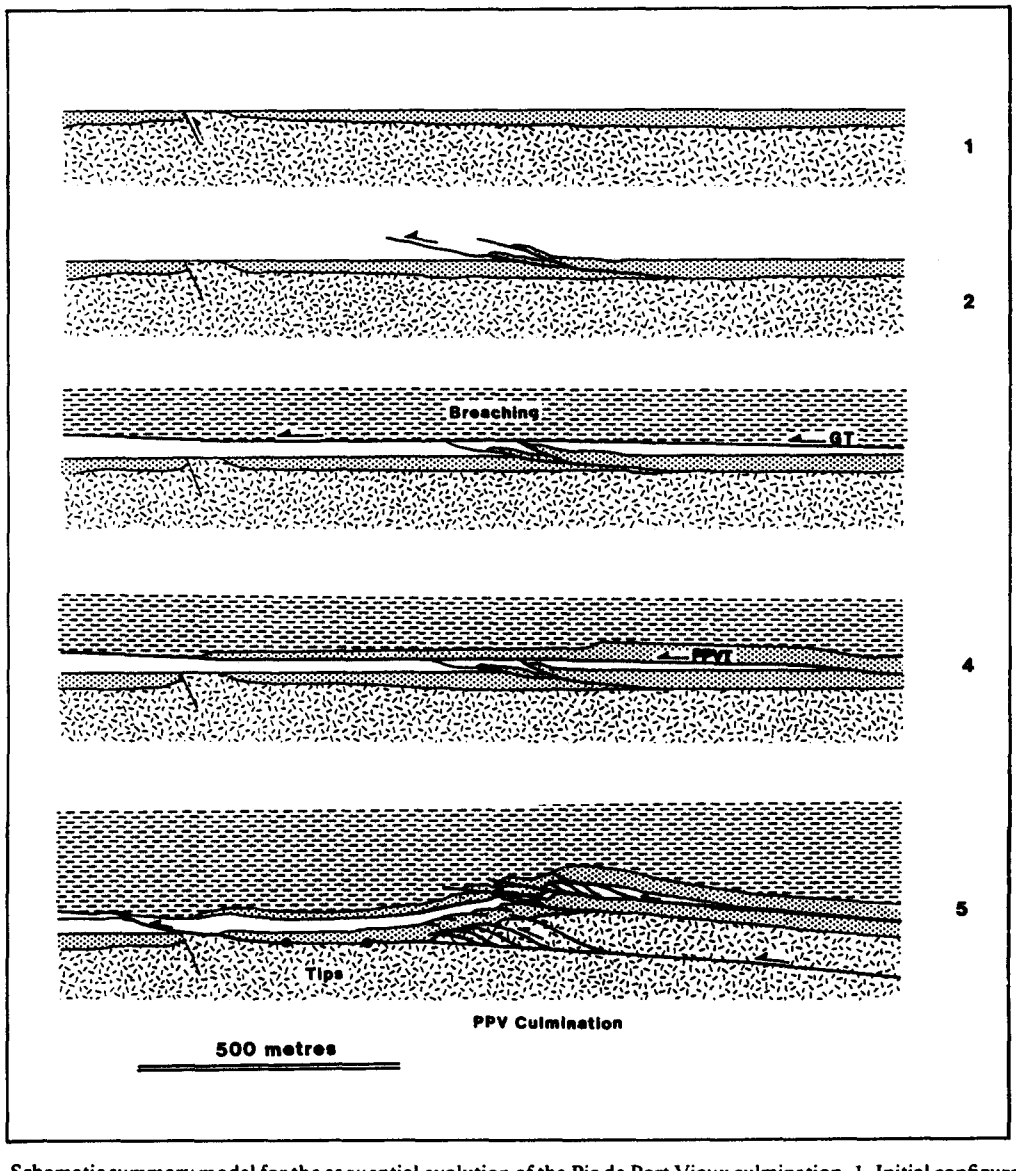

Fig. 5. Schematic summary model for the sequential evolution of the Pic de Port Vieux culmination. 1. Initial configuration. 2. Phase 1 thrusts locally imbricate the cover strata. 3 and 4. Emplacement of the Gavarnie and Pic de Port Vieux thrusts (phase 2 thrusts). These breach the phase 1 thrusts. 5. Development of the phase 3 structures produce the culmination.

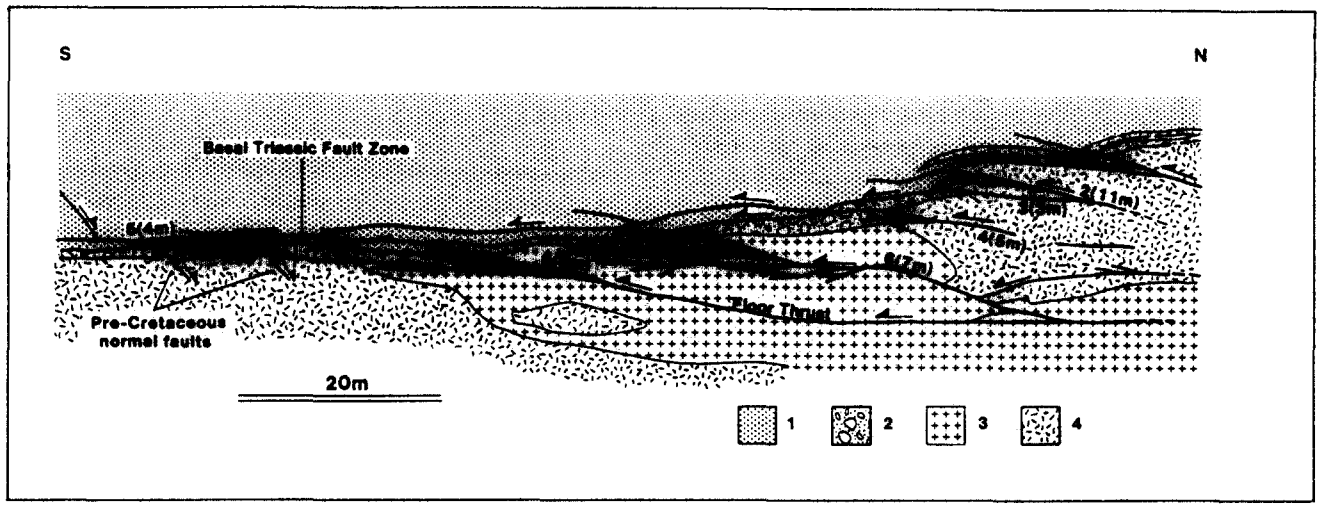

Fig. 6. Cross-section through the basement imbricate stack and the Basal Triassic fault zone. 1. Cleaved Triassic mudstone. 2. Basal Triassic conglomerate. 3. Granodiorite. 4. Hercynian metasediments. The displacements on some of the thrusts are shown by the bracketed numbers.

The cleavage in the Triassic strata refracts from the sandstone units into the shale beds. It also refracts through the thicker shale units where it possesses an overall sigmoidal form (Fig. 4). In addition, the strike of the cleavage varies across minor bedding-parallel faults and along the transport direction in the hangingwall of these minor faults. The minor faults probably formed in response to the shearing associated with emplacement of the two larger thrusts. The local strain state in the Triassic strata cannot, however, correspond to bedding-parallel simple shear because of the variable cleavage attitudes associated with the minor faults. The changes in cleavage attitude appear to reflect layer-parallel shortening and layer-normal shear strains associated with differential movement on individual bedding-parallel faults (e.g. Sanderson 1982, Coward & Potts 1983).

Phase 3 thrusts (P3)

The phase 3 (P3) thrusts are classified as faults that folded the PPVT during their propagation and movement. They record a switch in the locus of the deformation to the strata in the footwall of the PPVT. The main P3 structure is the Basement Imbricate Stack (BIS) (Fig. 2). It is composed of at least six imbricate thrusts that branch from a subhorizontal décollement within the Hercynian basement. The splays ramp steeply across the basal Triassic conglomerate and appear to flatten into the overlying mudstones. Where the floor fault cuts the unconformity it bifurcates into an anastomosing fault zone above the main basal conglomerate unit (Fig. 6). This fault zone will be referred to as the Basal Triassic fault zone (BTFZ).

The displacement on the thrusts in the BIS is constrained largely from the offset of the Triassic unconformity. The measured or estimated displacements are shown in Fig. 6. The direction of these displacements is towards the south (Fig. 7a). The cumulative displacement on the linked splays (excluding fault 6 which breaches the floor thrust) is between 40 and 45 m. The displacement in the BTFZ is 6 m and is constrained by the offset of two earlier normal faults that are cut by the zone. The imbricate splays do not link to the set of isolated thrusts that outcrop above the BIS (Fig. 2), and they appear to lose displacement within the Triassic mudstones. Accordingly, the structure is not a duplex but is a leading imbricate stack (Boyer & Elliott 1982).

The Triassic strata in the BIS possess a strong slaty cleavage which passes into a spaced anastomosing fabric in the basal conglomerate layer. The slaty cleavage is deformed by the BTFZ and changes in attitude across this structure: the cleavage is rotated approximately 25° clockwise and increases in dip by 5° in the hangingwall relative to the footwall of the fault zone (compare Figs. 7b & c). The significance of this reorientation will be discussed later.

The strata above the BIS possess a number of fault–fold structures (Fig. 2). Two of these structures are particularly important: (1) the Lower–Middle Fold Structure; and (2) the Upper Fold Structure and Upper Duplex (Fig. 2). An understanding of how they formed is critical to unravelling the complicated deformation sequence in the culmination.

The Lower–Middle Fold Structure

A set of isolated faults occurs within the Triassic strata above the BIS (Fig. 2). These faults have low angles of dip although they truncate strata that are tilted steeply westwards by the development of the BIS. The faults possess both trailing and leading tips, the latter forming folds along the Cretaceous unconformity. The Lower–Middle Fold Structure is associated with two of these tip folds. A detailed section through the structures is shown in Fig. 8.

The Lower Fold Structure (LFS) is a mesoscopic tip fold formed by one of the discontinuous thrusts (fault B in Fig. 8). The tip fold deforms the overlying PPVT and GT and also an earlier thrust labelled fault A. The

Middle Fold Structure (MFS) is formed by two phase 3 thrusts (faults D and E) that cut across a phase 1 thrust (fault P1A–P1B) and branch onto and fold the PPVT.

Fault B cuts across a set of folds in the strata adjacent to the Cretaceous unconformity. These folds become more asymmetrical downwards before dying out into layer-parallel shortening in the Triassic mudstones. Fault B splays into a number of secondary thrusts towards its tip. The splay labelled 1 (Fig. 8 inset) branches downwards from the subhorizontal splay labelled 2, but is not an extensional fault as it cuts up-section across the earlier folds. Restoration of the fault returns point V to point W and it therefore appears that splay 1 was folded prior to being cut across by splay 2. This geometry suggests that the folding both pre-dated and post-dated the initial development of fault B.

In the overlying PPVT sheet, the forelimb of the fold is cut by a complex array of minor thrusts that is absent from the undeformed limbs of the fold. This array comprises forethrusts which cut across high-angle faults that downthrow to the north. Five main forethrusts can be identified (Fig. 8). Only the fault labelled 4 actually breaches the PPVT and the others appear to branch from the folded thrust. Fault C (Fig. 8) is a large splay from the PPVT that cut across the crest of the fold and emplaced Triassic strata over the Silurian phyllite of the GT sheet. A smaller splay of similar geometry cuts across another fold in the PPVT at point X.

Thrusts such as fault C, which cut across the crestal points of folds in their own surfaces will be referred to as *back-limb splays* (BLS). These are to be distinguished from back-limb thrusts (Dahlstrom 1970, p. 341), which are thrusts that cut across the back-limb of an earlier fold but have not branched from a thrust that was folded by the earlier fold. Other back-limb splays are developed at X and Y in Fig. 8 while splay 2 at the tip of fault B and the fault labelled G that splays from the PPVT across the Middle Fold Structure can be similarly classified.

Back-limb splay fault C has an estimated displacement of 20 m. This displacement is greater than can be explained even if the observed displacements on faults B (approximately 12 m), D + E (3 m) and fault F (3 m) were transferred in total onto the PPVT. This discrepancy points to the existence of additional displacement on the PPVT. This can best be explained by postulating that upper detachments developed during the shortening responsible for cleavage development in the footwall strata. The presence of these detachments can also explain the back-limb splays. This inference is supported by an orientation analysis of cleavage in the structure. Data are shown in Figs. 9(a)–(e). The cleavage in the PPVT sheet is folded about a N–S axis (Fig. 9a) in contrast to the cleavage in the footwall of the thrust (both in the Cretaceous limestone and in the Triassic red beds) which dips NE at 45–55° (Figs. 9b & c). The folding of the cleavage in the PPVT sheet contrasts with the folding of the PPVT itself (Fig. 9d) or folding of the Triassic strata (Fig. 9e), both of which have NW–SE axes. It can be most easily explained as a product of movement over the nonplanar surface of back-limb splay C.

Mineral-fibre lineations on the faults in the LFS and MFS are shown in Figs. 9(f) & (g). Both fault B and the splays from the PPVT sheet possess bimodal lineation patterns. In both cases cross-cutting and curved relationships between shear fibres on the fault surfaces consistently indicate that the 160–170° azimuth was the later. Stretching lineations on the cleavage in the limestone record the same movement direction as the first movement azimuth on the faults. Note that this azimuth lies clockwise from the regional N–S movement vector.

The Upper Fold Structure and Upper Duplex

These two structures occur 50 m north of the MFS (Fig. 2b). An approximate transport-parallel section through the two structures is shown in Fig. 10.

The Upper Duplex comprises a set of at least six thrusts that shorten the Cretaceous strata. These thrusts splay from a floor thrust that approximately coincides

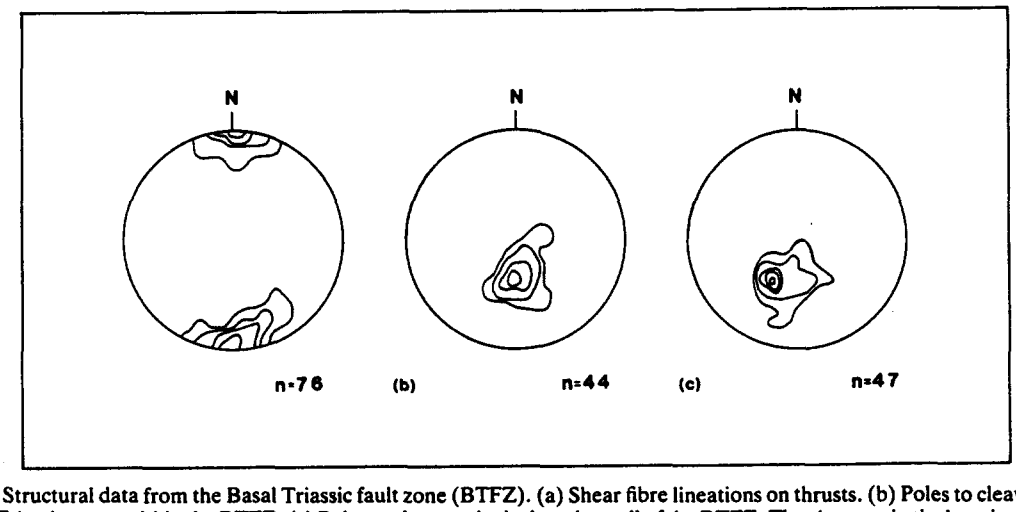

Fig. 7. Structural data from the Basal Triassic fault zone (BTFZ). (a) Shear fibre lineations on thrusts. (b) Poles to cleavage in the Triassic strata within the BTFZ. (c) Poles to cleavage in the hangingwall of the BTFZ. The cleavage in the hangingwall is rotated clockwise and possesses a steeper dip than the cleavage within (and cut by) the fault zone. Stereonets are contoured by hand at intervals of 5% per 1% area.

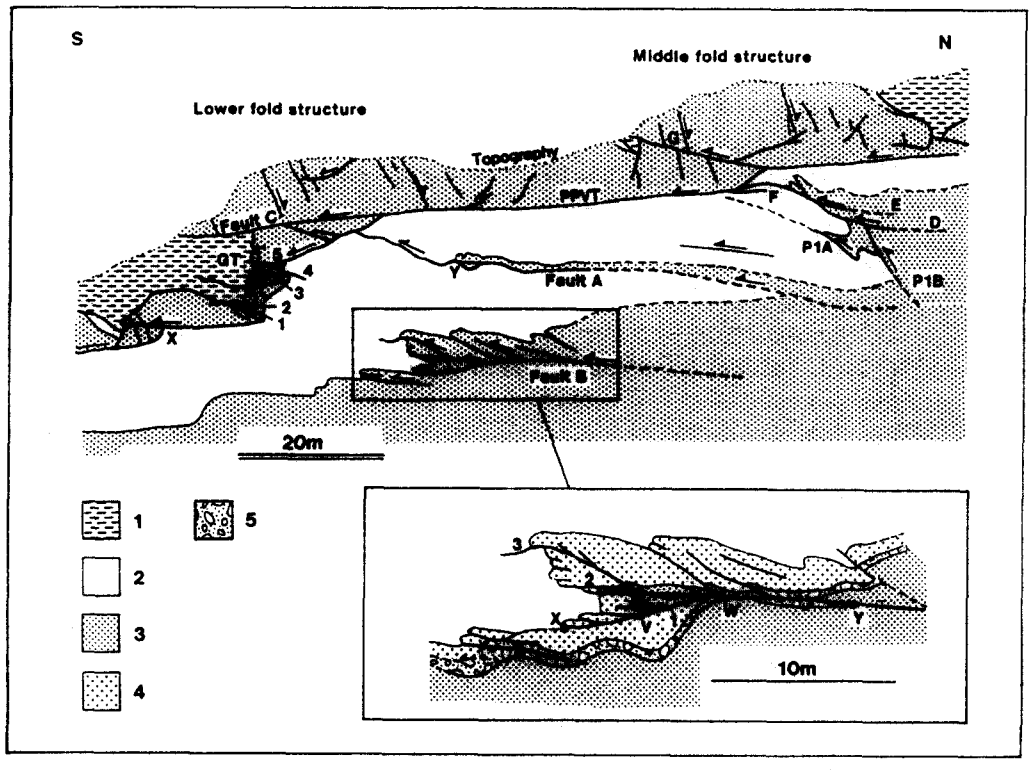

Fig. 8. N–S section through the Lower and Middle Fold Structures. The inset shows the tip fold associated with fault B in more detail. 1. Silurian phyllite. 2. Cretaceous limestone. 3. Triassic red beds. 4. Dolomitic sandstone. 5. Dolomitic pebble conglomerate. 4 and 5 represent base-Cretaceous strata although they have been grouped as part of the Triassic in the main section. This has been done solely to emphasize the form of the structures. See text for discussion.

with the Cretaceous unconformity. All the thrusts join the PPVT apart from fault 2, which breaches the roof thrust at the crest of the structure, and fault 6, which cuts across the crest of an earlier formed monocline to breach the PPVT at the front of the structure. Fault 6 is a back-limb thrust with respect to the monocline and splits into a set of en échelon faults above the fold crest. These faults deform the cleavage in the limestone in contrast to the other thrusts in the duplex, which are sub-parallel to cleavage. The frontal portion of the Upper Duplex constitutes the Upper Fold Structure (UFS).

Three thrusts breach the PPVT in the UFS and are labelled J, K and L (Fig. 10). Fault J occurs structurally below the floor thrust of the Upper Duplex (fault K) and is probably an out-of-the-syncline thrust (Dahlstrom 1970) associated with the shortening that produced the monocline. Fault L is a discontinuous thrust that steps up from the level of fault K and is the upper fault of the en échelon array in the limestone. This array appears to represent a discontinuous ramp, movement on which folded the splay from the PPVT labelled M. Fault M places the PPVT sheet over the Silurian phyllite of the GT sheet and restores to a back-limb splay that formed across the initial monocline. Fault N (Fig. 10) is a later BLS that cut across the crest of the folded fault M.

The attitude of cleavage in the Upper Duplex is shown in Fig. 11. The cleavage does not change orientation systematically across individual thrusts but progressively rotates clockwise accompanied by an increase in dip towards the front of the structure. Only fault 6 clearly deforms the cleavage. This suggests that the oblique cleavage development post-dated movement on some thrusts but pre-dated movement on others. The duplex therefore appears to have had two phases of movement, the latter phase restricted to fault 6 at the front of the structure.

The shear fibre lineations associated with the faults in the Upper Duplex are shown in Figs. 9(h) & (i). Both the en échelon secondary faults within the limestone and the BLS from the PPVT (faults M and N) possess bimodal lineation patterns identical to those described for the LFS. In addition extension fibres from veins associated with the tips of the secondary faults have the same pattern. These veins appear to have dilated parallel to the slip on the faults, and cross-cutting relationships between the vein sets and between the shear fibres on the faults indicate that the SSE movement vector was the later.

Fault rocks associated with P3 thrusts

The phase 3 thrusts within the basement and Triassic strata of the PPV culmination are discrete fractures coated with layers of quartz–chlorite shear fibres. There is no significant difference in the nature of these fault rocks between small displacement (<1 m) and larger displacement (>5 m) faults. Inclusion bands within the fibres indicate that they grew by a crack–seal mechanism (Ramsay 1980). Fault-parallel cavities are also common along a number of thrusts in the culmination and are locally developed within the basal Triassic fault zone, along fault B in the Lower Fold Structure, along a

number of back-limb splays in the PPVT sheet, and along some of the low-angle normal faults that are also present within the PPVT sheet (see Fig. 10). All the cavities have a similar appearance and are elongate planar or irregular veins filled with randomly oriented euhedral crystals of quartz. These crystals grow in layers within the cavities that signify different dilation episodes (Grant 1989). The presence of jigsaw-pattern fractured shale clasts within the cavities suggests the cavities owe their origin to the localized and possibly rapid hydraulic jacking open of the fault planes. Fault cavities are absent from thrusts affecting the Triassic strata outside the culmination.

Lineation distributions on the phase 3 thrusts

Many of the phase 3 thrusts that formed directly in the footwall of, and also within, the PPVT sheet possess bimodal shear fibre lineation distributions. This type of distribution is absent from the thrusts within the BIS (compare Fig. 7a with Figs. 9f & g). The first formed lineation is directed either S or SSW. The second lineation is consistently directed SSE and always cuts the first. The second lineation appears to record a late-stage movement event that probably occurred simultaneously on the faults affected. This event appears to represent a localized distributed shearing along the base of the PPVT–GT. This shearing did not affect the structures in the BIS–BTFZ.

DISCUSSION

Fault sequence in the culmination

The thrust sequence in the PPV culmination (P1–P3) is not foreland propagating as it is complicated by both the breaching involved in the emplacement of the GT and by the development of isolated thrusts above the leading tip of the BIS. The PPVT, Upper Duplex and the BIS did form however in a straight-forward piggy-back sequence.

Neglecting the GT, the main complications in the thrust sequence occurred as a result of re-activation of some of the thrusts during the folding associated with the growth of the BIS. This re-activation appears to have occurred intermittently. For example, fault B (Fig. 8) appears to have had two movement episodes between

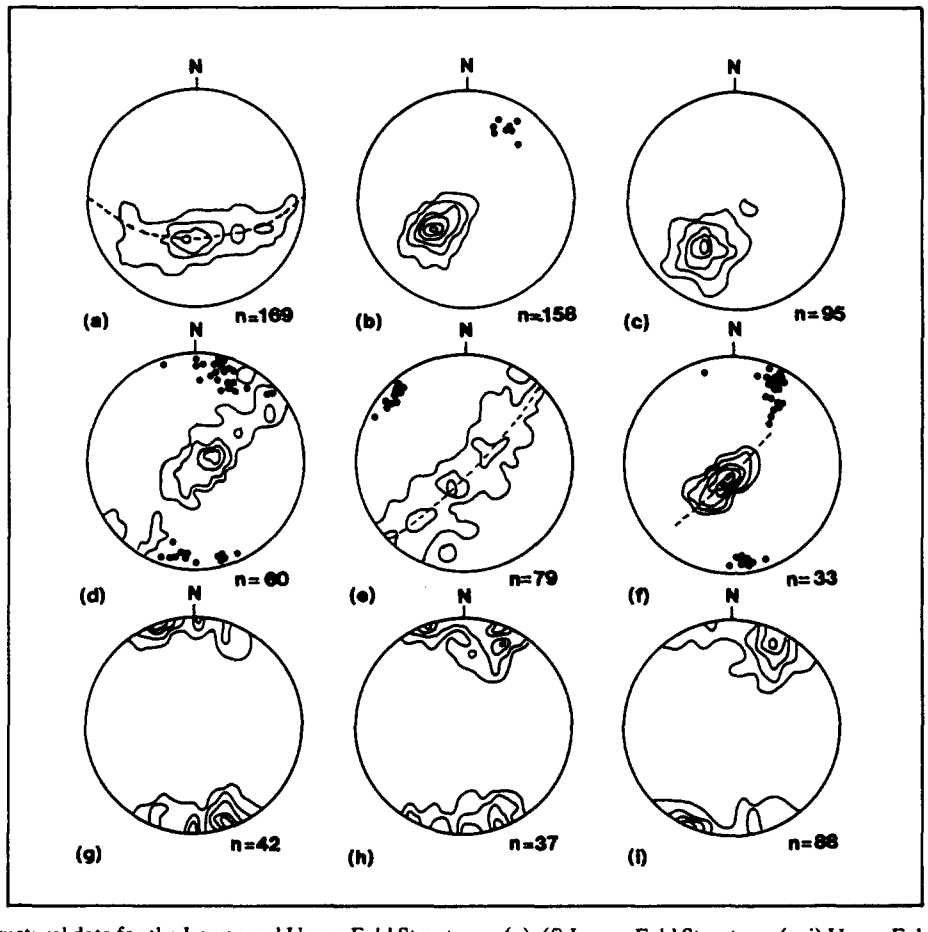

Fig. 9. Structural data for the Lower and Upper Fold Structures. (a)–(f) Lower Fold Structure; (g–i) Upper Fold Structure. (a) Poles to cleavage in the PPVT sheet. (b) Poles to cleavage and stretching lineations (dots) in the Cretaceous limestone. (c) Poles to cleavage in the Triassic strata. (d) Poles to the PPVT and shear fibre lineations on the thrust and the back-limb splays. (e) Poles to bedding in the Triassic strata and fold axes (dots). (f) Poles to fault B and shear fibre lineations on the fault (dots). (g) Shear fibre lineations on the PPVT. (h) Shear fibre lineations on thrusts within the Cretaceous limestone. (i) Extension fibres from tension gashes associated with the faults in the Cretaceous limestone. Fault B, the PPVT and back-limb splays in both fold structures and the secondary faults in the limestone of the Upper Fold Structure all possess bimodal lineation patterns. Contours are at 5% intervals.

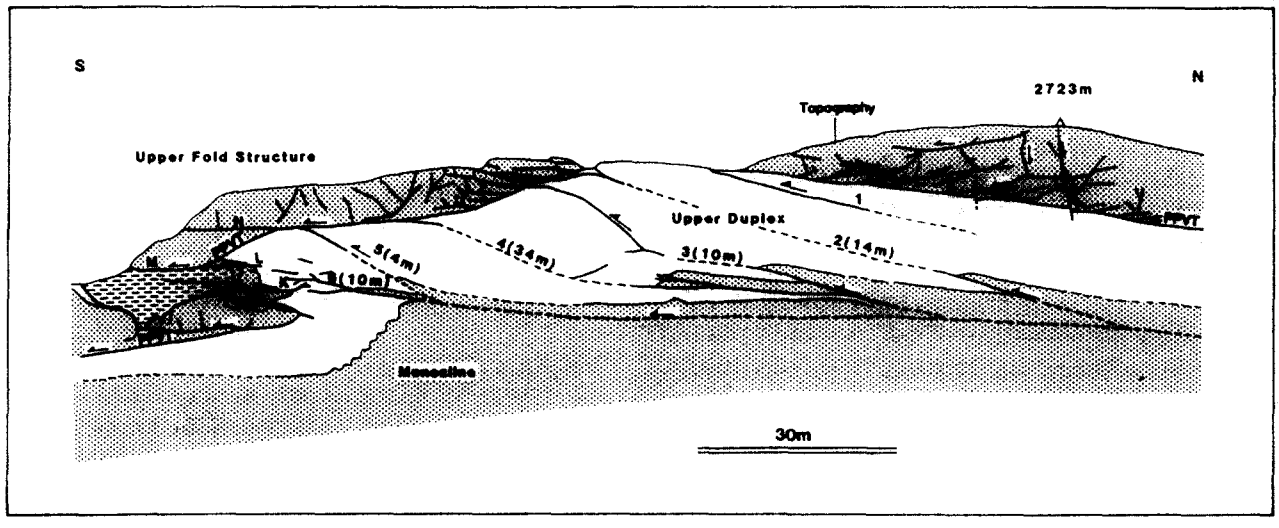

Fig. 10. Cross-section through the Upper Fold Structure and Upper Duplex. Estimated displacements on the thrusts in the Upper Duplex are given in brackets.

which it (splay 1) was gently folded. Similarly, the PPVT in the Lower Fold Structure appears to have re-activated at least twice, first associated with the fold train along the unconformity (this accounts for back-limb splays X and 1, 2, 3 marked in Fig. 8) and then associated with the tip fold produced by movement on fault B (accounting for BLS splay 5 and fault C). A similar argument can also be applied to the Upper Fold Structure where the PPVT was re-activated subsequent to the formation of the monocline (fault M) and then subsequent to the folding of fault M by the re-activation of the leading fault of the Upper Duplex (splay 6 in Fig. 10) forming BLS fault N.

The movements of individual faults and back-limb splays appears to be out-of-sequence with regard to the individual structures concerned. It can, however, be considered in-sequence with the formation of the BIS because the movements are related to the overall shortening associated with this structure via development of localized upper detachments. Two phenomena are therefore being recorded: (1) episodic development of

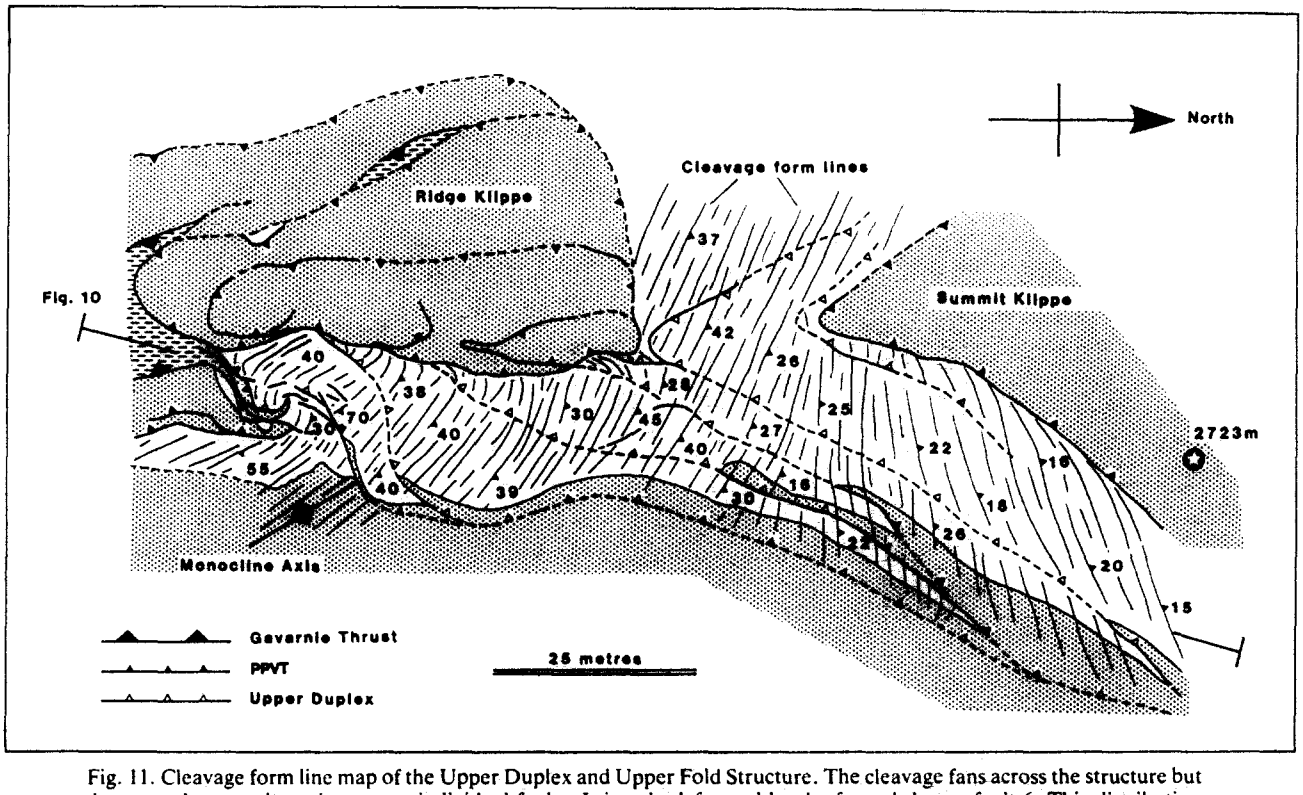

Fig. 11. Cleavage form line map of the Upper Duplex and Upper Fold Structure. The cleavage fans across the structure but does not change orientation across individual faults. It is only deformed by the frontal thrust, fault 6. This distribution suggests that the duplex pre-dated the development of the cleavage fan but that the frontal thrust was later re-activated. The rotation of the cleavage indicates an increasing dextral layer-normal shear component in the deformation towards the front of the structure. This component is related to the oblique fault tips developed in the basement imbricate stack.

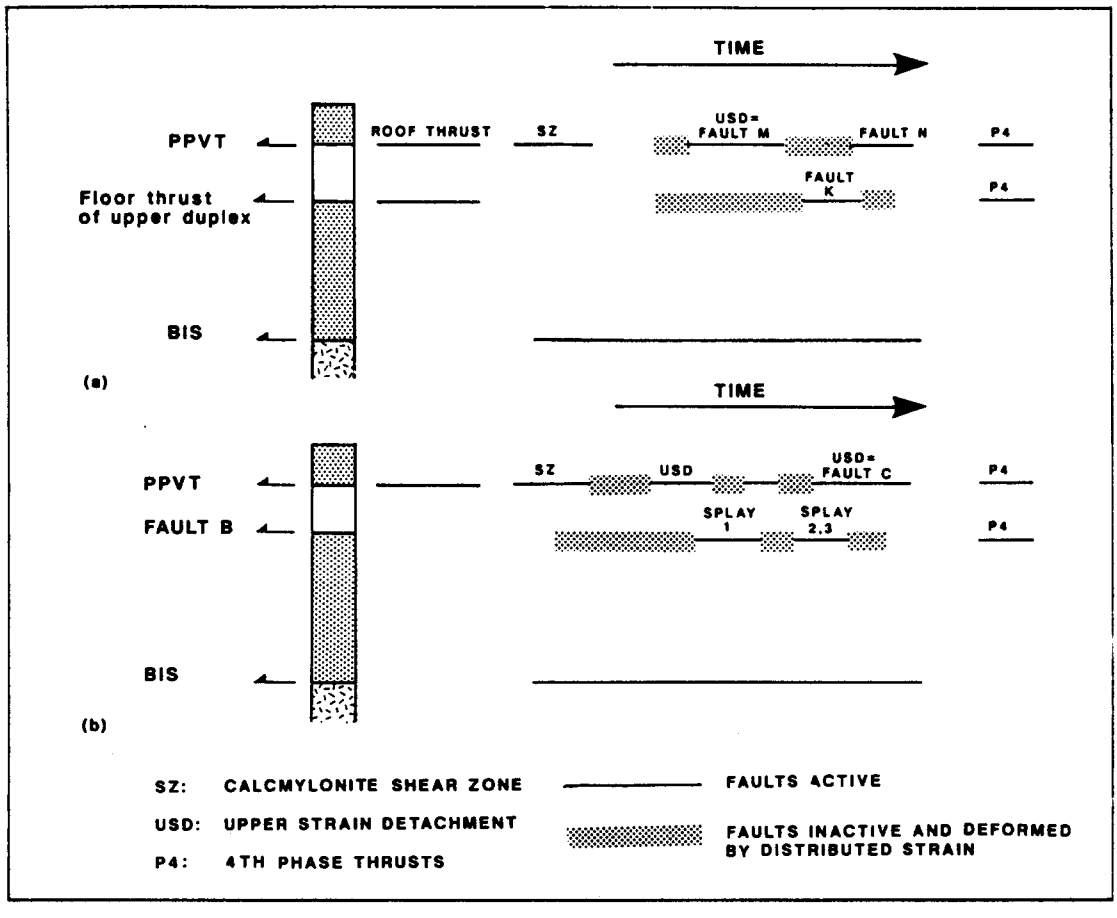

Fig. 12. Fault movement–time diagrams for the Upper Duplex (a) and the Lower Fold Structure (b). Time is plotted horizontally and the relative physical position of the thrusts plotted vertically. A line represents fault activity (localized deformation), the dotted strips represent periods when the faults are inactive or have not yet formed and the rock is deforming by cleavage development (distributed deformation). The time scale is only qualitative but is considered similar for each structure. The sequence of fault movements has been worked out from superposition of structures. In both cases the PPVT has had a multiple movement history. It was initially active as the roof thrust to the upper duplex before the fault activity switched to the BIS. During shortening in the BIS, the PPVT was re-activated, first as a calc-mylonite shear zone in the Cretaceous limestone, and then as localized back-limb splays associated with the development of upper strain detachments. Fault B in the Lower Fold Structure and fault K in the Upper Fold Structure were also re-activated late in the deformation history (they deform cleavage and cut across earlier formed folds). The diagram portrays the diachronous movements of faults in the strata above the BIS. Note that the distributed deformation in the upper duplex is modelled as commencing slightly later than in the Lower Fold Structure. This is because as the faults locked up, the intensity of the tip strain would probably have propagated backwards from the front of the structure (see Fig. 14).

upper detachments on faults; and (2) a diachroneity in the fault movement caused by the intermittent reactivation of the detachments. By changing the scale of observation an out-of-sequence thrust with respect to one structure can become an in-sequence thrust with respect to another that was responsible for the first during a progressive deformation. This can be portrayed in the form of fault movement–time plots for the structures (Fig. 12). Because the fold structures do not interfere it is difficult to determine their relative age. The fact that in each the faults deform the cleavage in the culmination and were also deformed by further distributed deformation suggests that the structures formed simultaneously.

Cleavage obliquity in the culmination

The cleavage in the Triassic and Cretaceous strata in the PPV culmination is oriented 45° clockwise oblique to that expected for the N–S transport recorded by shear fibre lineations in the BIS and BTFZ. In addition, the cleavage fans from SE–NW to E–W towards the rear of the Upper Duplex (Fig. 11) and a similar fanning, but of opposite polarity, occurs south of the culmination. Within the culmination, the change in cleavage strike is accompanied by an increase of the dip and increase of the intensity of the fabric.

The reorientation of cleavage in the culmination can be equated with both leading and lateral tip strain associated with the loss of displacement on the BIS thrusts. The increase in dip records layer-parallel shortening, whereas the rotation in cleavage strike records a dextral longitudinal shear component that reflects the oblique tipping of the thrusts. In addition to the rotation of cleavage, the first displacement vectors to form on the P3 thrusts above the BTFZ also appear to have been rotated clockwise from the regional N–S vector to NNE–SSW. The fact that the faults moved synchronously with cleavage development suggests, however, that the vectors were not physically rotated after they formed but

formed as a result of the rotation in the displacement field associated with the tip strain. This supports the pole of rotation model for fault displacement at a lateral tip (Coward 1984).

Cleavage–fault interaction

The distribution of cleavage and faults in the PPV culmination suggests that two fault–fold–fault transitions occur within the structure (Fig. 13). The first transition represents the change from displacement on the BIS thrusts to cleavage development in the Triassic strata and back to discontinuous displacements on the thrusts that formed adjacent to the Cretaceous unconformity. The second transition occurs across the cleaved Cretaceous limestone with shortening transferred back onto slip along the PPVT to form the back-limb splays.

A simplified model explaining how an upper detachment forms is shown in Fig. 14. The model requires the localization of a fault within a zone of distributed strain, the fault then propagating both forwards and backwards, transferring the zone of distributed strain in its hangingwall further towards the foreland. The discontinuous thrust probably localizes along or adjacent to a material inhomogeneity where differential stresses are likely to be high. In the PPV culmination this inhomogeneity appears to be represented by the main lithological boundaries between the Triassic red beds and Cretaceous limestone. The model is a modification of the "upper detachment in concentric folding" model of Dahlstrom (1970) with cleavage development taking the place of concentric folding.

It is not the space problem associated with folding that necessitates development of an upper detachment, but the rheological contrast between the different layers that are being shortened. This has been discussed by Morley (1987) who used a detachment model to explain vertical strain variations in the Osen–Røa thrust sheet. The presence of cusp folds and cleavage refraction in the fold structures in their PPV culmination suggests that the Cretaceous limestone behaved as the more competent unit during shortening.

Controls on episodic fault movement

It has been shown that in the PPV culmination, upper detachments operated episodically with periods of fault slip (development of back-limb splays) interspersed with periods during which the faults behaved passively and were folded. The intensity of different strain accommodation mechanisms therefore varied temporally as well as spatially within the culmination. This produced the observed diachroneity of fault movement history.

The faults in the PPV culmination moved by a press-

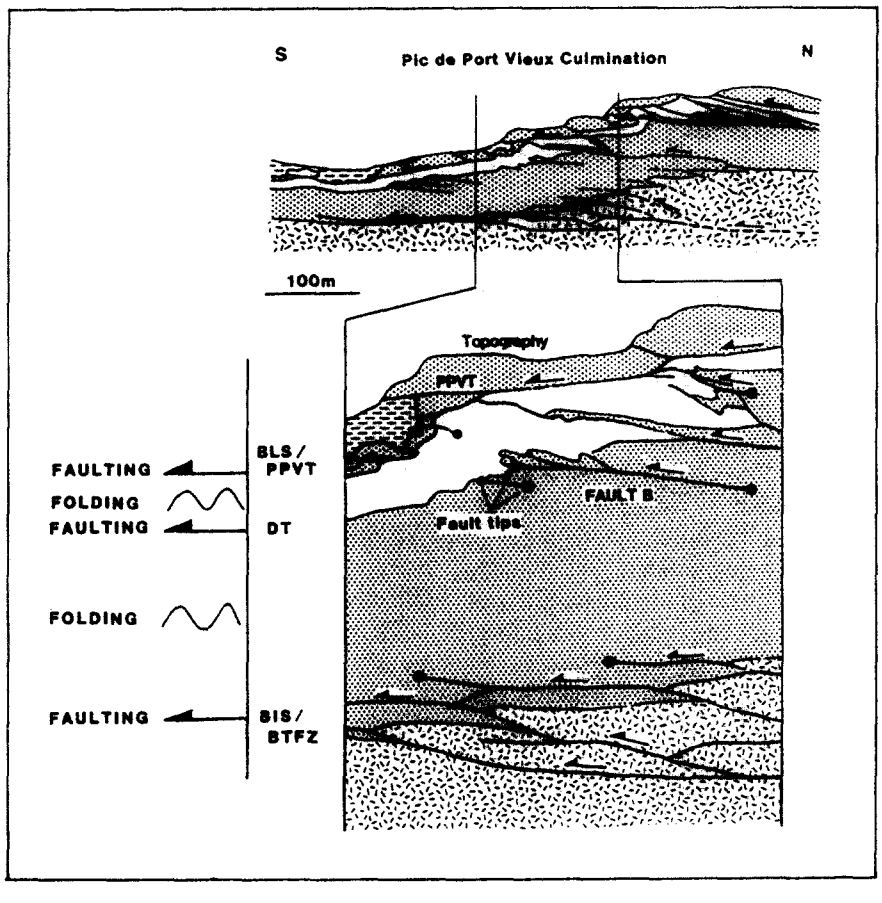

Fig. 13. Definition of the two fault–fold–fault transitions in the PPV culmination. The transitions occur across both the Triassic cleaved shales and the Cretaceous limestone above the BIS. The detachments occur adjacent to the main lithological and structural boundaries and suggest that these played an important role in localizing thrusts. The contacts were folded prior to the development of the upper detachments and thus changed from passive to active during the deformation. DT: discontinuous thrusts.

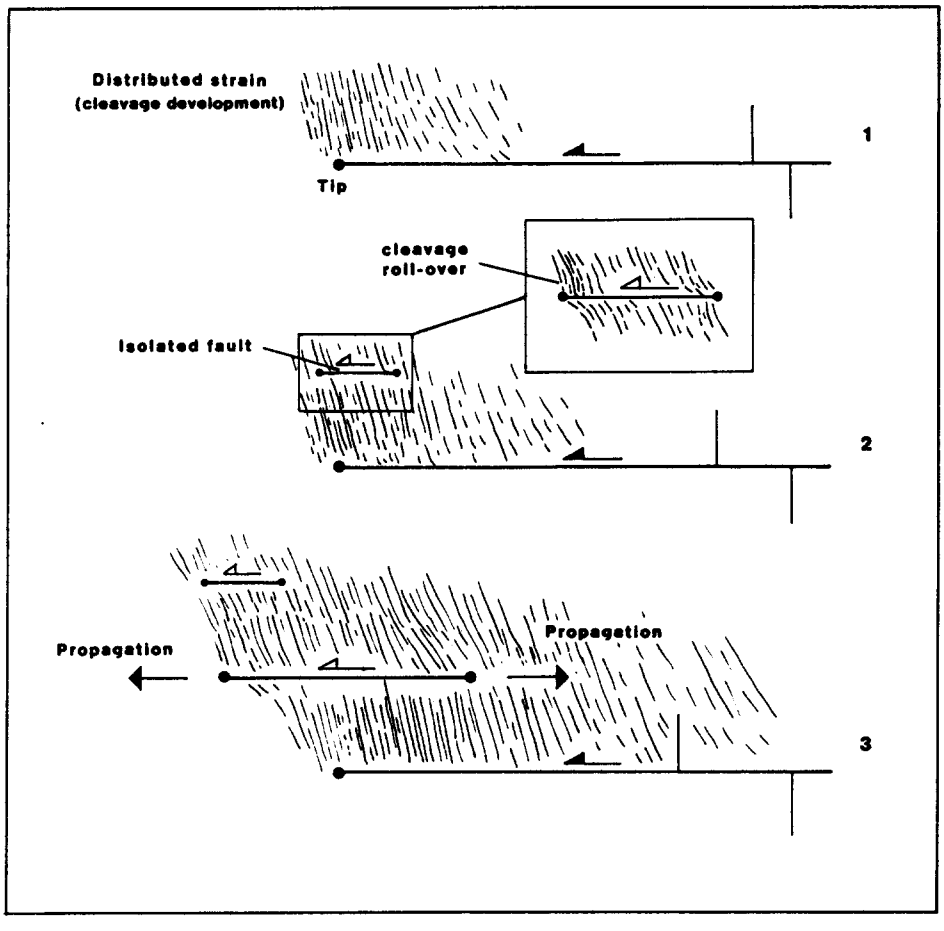

Fig. 14. Model for an upper detachment. 1. A zone of distributed strain develops at the tip of a fault. 2. At some stage in the deformation a small fault localizes within the tip zone. This fault deforms the earlier cleavage (see inset). 3. The discontinuous fault propagates both forwards and backwards as displacement on the lower fault continues. This has the effect of transferring the zone of shortening further towards the foreland.

ure solution–precipitation displacement mechanism that was responsible for the growth of crack–seal fibre packets along the fault planes. This type of movement mechanism involved repeated slip increments of dimensions between 10 and 50 μm, corresponding to the widths of crack–seal inclusion bands. The slip increments were accompanied presumably by periods during which healing–sealing of the microfractures took place. The overall movement history therefore involved a sort of regular (steady-state) stick–slip (Gaviglio 1986) in which the extensional fracturing of the fault plane shear-fibre-packet accompanied the slip phase and healing–sealing of the microfractures accompanied the stick portion of the cycle. Individual episodes of this type of slip allowed up to 10–20 m of displacement on the detachments to accumulate.

The mechanical stratigraphy in the culmination appears to have influenced the location of the detachments, but it was presumably the local environmental conditions that influenced their episodic movement history. Possible environmental candidates require to be parameters that could have fluctuated both spatially and temporally during the progressive deformation. The existence of high fluid pressures during the deformation is indicated by the presence of fault-parallel cavities, and fluid pressure cycling is recorded by the incremental opening and sealing of these cavities. It is attractive therefore to consider that fluid overpressure was the main parameter that controlled the fault slip history.

If fluid pressure cycling was responsible for the fault slip history it probably did so by a positive feedback process in association with fault-related dilatancy (Fig. 15).

(1) Build up of fluid pressures in the culmination probably occurred in response to the distributed deformation. Mathematical modelling by Walder & Nur (1984) and Cello & Nur (1988) has shown that inelastic porosity reduction (by pore compressibility, mineral precipitation and/or DMT processes) can rapidly generate fluid overpressures. The low intrinsic permeability of the fine-grained low-porosity Triassic and Cretaceous strata would have facilitated the generation of the very high fluid pressures required to hydrofracture the faults. The absence of fault cavities along thrusts outside of the culmination (outside the locus of distributed deformation) supports this model as it requires the operation of a local rather than regional overpressuring mechanism. Assuming the faults moved aseismically (this is probably in accordance with the described slip mechanism) implies that the seismic pumping mechanism (Sibson *et al.* 1975) did not operate in the fault system during P3 thrusting. Channelized fluid flow appears to have

occurred during fault slip episodes and is recorded by compositional variations in cavity-fill chlorites. These chlorites possess μm-scale compositional zones that record expulsion of fluid from the Cretaceous limestone into the Triassic red beds (Grant 1989) during hydrofracture episodes. The study of these chlorites will be the subject of a separate paper.

(2) The increase in ambient fluid pressure effectively weakened the rock by decreasing the effective stresses in the deforming strata. This enabled fracturing to develop (detachments to nucleate or earlier thrusts to reactivate) along or adjacent to the main lithological boundaries where differential stresses were presumably greatest during the deformation (e.g. Schedl & Wiltschko 1987).

(3) Microfracturing and vein formation associated with fault movement increased local permeability and probably allowed fluid pressures to drop via drainage. In areas where drainage was restricted the dilatancy associated with fracturing may also have contributed to the pressure drop. Such a phenomenon has been shown by Teufel (1980, 1981) to occur in simulated stick–slip faulting. The fracture dilatancy can in addition act as a fluid pumping mechanism (Etheridge *et al.* 1984, Cox & Etheridge 1989). The mechanical effect of a reduction in fluid pressure in the volume surrounding a fault will be an increase in the stiffness of the medium (Rice & Simmons 1976, Rudnicki 1980). This will either stabilize fault slip or, more likely for the aseismic faults documented here, have arrested fault movement.

(4) The episodes of fault slip occurred during distributed deformation in the surrounding strata. When slip was arrested, the passive faults were then buckled by continued bulk penetrative shortening. After sufficient fluid pressure buildup the next slip episode was activated and a back-limb splay developed from the folded fault.

As already mentioned, the duration of the slip episodes was such that displacements of between 3 and 20 m accumulated on individual back-limb splays. This points to the persistence of the fluid overpressuring in the system during localized fault activity; that is, fluid pressure dissipation was slow. This behaviour can be expected considering the low permeability of the strata. The restriction of zoned cavity-fill chlorites to fault cavities suggest that it was only during the hydrofracture events that major channellized fluid flow and, by inference, fluid expulsion occurred from the lithostatically pressured volume of deforming rock in the culmination. It is possible that major slip arrestment accompanied these hydrofracture episodes when rapid drainage occurred from the system. This is supported by the observation that the quartz–chlorite fill in cavities along some of the detachments is undeformed; that is, further fault slip did not occur after the cavities formed. In other cavities, however, the cavity fill has been deformed by later slip episodes.

The model described here therefore envisages a close relationship between fluid pressures and fault activity to the extent that fault slip episodes were controlled by fluid pressure fluctuations. The fluid pressures are therefore considered not only to have controlled the rock response to deformation but ultimately the type of deformation mechanisms that operated and their temporal distribution. The model is similar to the fault-valve model of Sibson *et al.* (1988) except that here it is applied to what are considered to be aseismic thrusts.

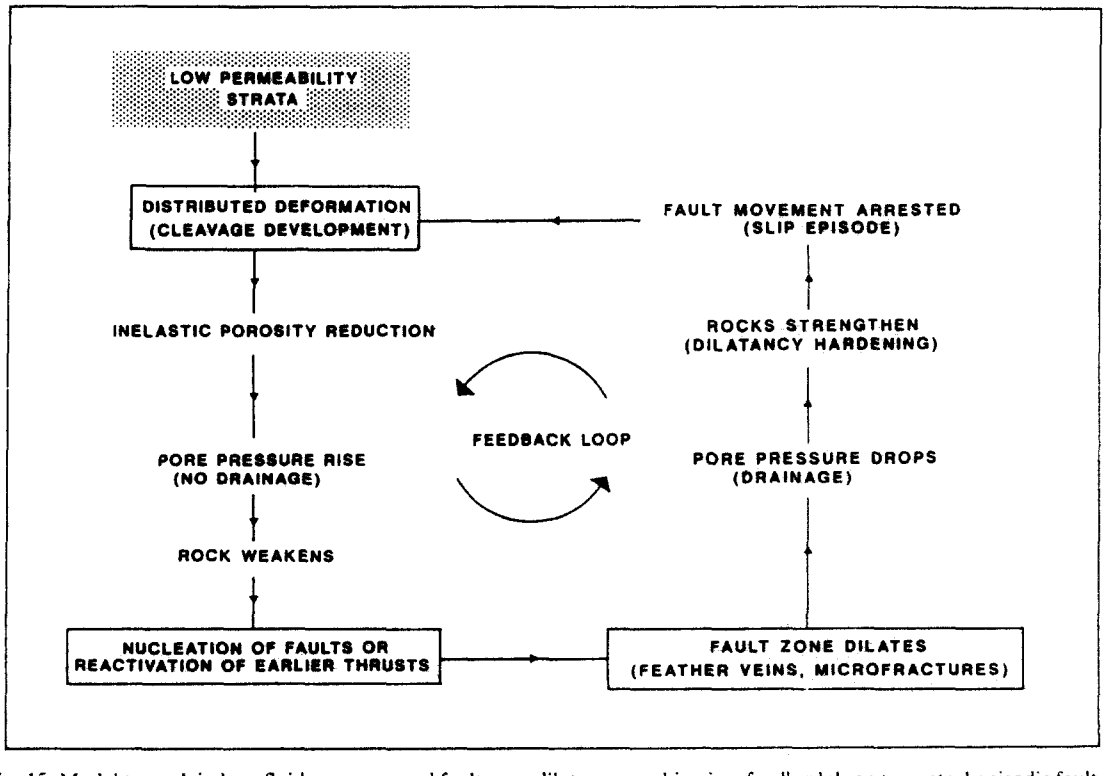

Fig. 15. Model to explain how fluid pressures and fault zone dilatancy combine in a feedback loop to control episodic fault activity. See text for discussion.

CONCLUSIONS

Detailed mapping of a thrust culmination in the central Pyrenees (the Pic de Port Vieux culmination) has revealed a complex fault sequence produced by the interaction of thrusts and distributed strain. This interaction has resulted in temporal changes in the deformation with episodes of discrete deformation (fault slip) interspersed with episodes of distributed deformation where bulk shortening dominated. The main control on this history appears to have been exerted by fluid pressure fluctuations within the structure during deformation. New faults formed or old thrusts were reactivated during periods when near-lithostatic fluid pressures existed in the culmination. These overpressures were probably generated by cleavage development in the low permeability Triassic and Cretaceous strata deformed in the culmination. The reactivation of earlier thrusts produced upper detachments in the structure that produced fault–fold–fault transitions across the main stratigraphic units. The main detachment occurred along the roof thrust and was localized to the back-limbs of folds in the thrust, producing splays that cut across the fold crests. Movement on these detachments can be shown to have been episodic, and when inactive the faults were folded. The later movements on the detachments occurred on new back-limb splays, and led locally to a break-back splay sequence. Fault slip episodes appear to have terminated abruptly when the lithostatic fluid pressures were relieved by channelized fluid expulsion from the structure during hydrofracture events. These events produced a high-permeability fault-parallel cavity network that enabled drainage to occur. Continued deformation subsequent to cavity sealing then resulted in the next cycle of fluid pressurization and the next slip episode on the detachments.

Acknowledgements—This work was completed as part of the requirements for a NERC funded Ph.D. at Leeds University. I would like to express my gratitude to Mr Fred Faget and family for their support and friendship during completion of my field work and to Dr Andy McCaig, Dr John Platt and Sarah Curtis for valuable discussion and comments during the preparation of this paper. Healthy critiques by Chris Morley and Michael Ellis greatly improved the first draft of the text. This work was first presented at the Tectonic Studies Group AGM in Hull in 1986.

REFERENCES

Banda, E. & Wickham, S. M. 1986. The geological evolution of the Pyrenees—an introduction. *Tectonophysics* **129**, 1–8.

Boyer, S. E. & Elliott, D. 1982. Thrust systems. *Bull. Am. Ass. Petrol. Geol.* **66**, 1196–1230.

Cello, G. & Nur, A. 1988. Emplacement of foreland thrust systems. *Tectonophysics* **7**, 261–271.

Choukroune, P. & Seguret, M. 1973. Tectonics of the Pyrenees: role of compression and gravity. In: *Gravity and Tectonics* (edited by DeJong, K. H. & Schotten, R.). Wiley, New York, 141–156.

Coward, M. P. 1984. The strain and textural history of thin-skinned tectonic zones: examples from the Assynt region of the Moine Thrust Zone of Northwest Scotland. *J. Struct. Geol.* **6**, 89–99.

Coward, M. P. & Potts, G. J. 1983. Complex strain patterns developed at the frontal and lateral tips to shear zones and thrusts. *J. Struct. Geol.* **5**, 383–399.

Cox, S. F. & Etheridge, M. A. 1989. Coupled grain-scale dilatancy and mass transfer during deformation at high fluid pressures: example from Mount Lyell, Tasmania. *J. Struct. Geol.* **11**, 147–162.

Dahlstrom, C. D. A. 1969. Balanced cross sections. *Can. J. Earth Sci.* **6**, 743–757.

Dahlstrom, C. D. A. 1970. Structural geology in the eastern margin of the Canadian Rocky Mountains. *Bull. Can. Petrol. Geol.* **18**, 332–406.

Deramond, J., Joseph, J., Majeste-Menjoulas, C. & Mirouse, R. 1980. Geometrie des deformations dans une nappe complexe: La Nappe de Gavarnie (Pyrenees centrales, France). *Geol. Rdsch.* **69**, 659–677.

Deramond, J., Graham, R. H., Hossack, J. R., Baby, P. & Crouzet, G. 1985. Nouveau modele de la chaine des Pyrenees. *C.r. Acad. Sci., Paris* **2**, 1213–1216.

Etheridge, M. A., Wall, V. J. & Cox, S. F. 1984. High fluid pressures during regional metamorphism and deformation: implications for mass transport and deformation mechanisms. *J. geophys. Res.* **89**, 4344–4358.

Fischer, M. W. 1984. Thrust tectonics in the North Pyrenees. *J. Struct. Geol.* **6**, 721–726.

Fontbote, J. M., Muñoz, J. A. & Santanach, P. 1986. On the consistency of proposed models for the Pyrenees with the structure of the eastern part of the belt. In: *The Geological Evolution of the Pyrenees* (edited by Banda, E. & Wickham, S. M.). *Tectonophysics* **129**, 291–302.

Gaviglio, P. 1986. Crack–seal mechanisms in a limestone: a factor of deformation in strike-slip faulting. *Tectonophysics* **131**, 247–255.

Grant, N. T. 1989. Deformation and fluid processes in thrust sheets from the central Pyrenees. Unpublished Ph.D. thesis, University of Leeds.

Grant, N. T., Banks, D. A., McCaig, A. M. & Yardley, B. W. D. In press. The chemistry, source and behaviour of fluids involved in Alpine thrusting of the Central Pyrenees. *J. geophys. Res.*

Knipe, R. J. 1989. Deformation mechanisms—recognition from natural tectonites. *J. Struct. Geol.* **11**, 127–146.

Labaume, P., Seguret, M. & Seyve, C. 1985. Evolution of a turbiditic foreland basin and analogy with an accretionary prism: example of the Eocene South-Pyrenean Basin. *Tectonics* **4**, 661–665.

Lucas, C. 1985. Le Grès Rouge de versant nord des Pyrenees. Essai sur la géodynamique de depôts continentaux du Permien et du Trias. Unpublished Ph.D. thesis, University of Toulouse.

Martinez, A. 1968. Étude sructurale de la region de la Cinqueta—Substratum de la Nappe de Gavarnie (Pyrenees, Espagne). Unpublished thèse troisième cycle, University of Montpellier.

Mattauer, M. & Henry, J. 1974. The Pyrenees. In: *Mesozoic–Cenozoic Orogenic Belts* (edited by Spencer, A. M.). *Spec. Publs geol. Soc. Lond.* **4**. Scottish Academic Press.

Mitra, G. 1982. Brittle to ductile transition due to large strains along the White Rock thrust, Wind River mountains, Wyoming. *J. Struct. Geol.* **6**, 51–63.

Morley, C. K. 1987. Lateral and vertical changes of deformation style in the Osen–Røa thrust sheet, Oslo region. *J. Struct. Geol.* **9**, 331–343.

Muñoz, J. A., Martinez, A. & Verges, J. 1986. Thrust sequences in the eastern Spanish Pyrenees. *J. Struct. Geol.* **8**, 399–406.

Parish, M. 1984. A structural interpretation of a section of the Gavarnie Nappe and its implications for Pyrenean geology. *J. Struct. geol.* **6**, 247–255.

Ramsay, J. G. 1980. The crack–seal mechanism of rock deformation. *Nature* **284**, 135–140.

Rice, J. R. & Simmons, D. A. 1976. The stabilisation of spreading shear faults by coupled deformation–diffusion effects in fluid-infiltrated porous materials. *J. geophys. Res.* **81**, 5322–5334.

Rudnicki, J. W. 1980. Fracture mechanics applied to the Earth's crust. *Annu. Rev. Earth & Planet. Sci.* **8**, 489–525.

Sanderson, D. J. 1982. Models of strain variation in nappes and thrust sheets: a review. In: *Strain Within Thrust Belts* (edited by Williams, G. D.). *Tectonophysics* **88**, 201–233.

Schedl, A. & Wiltschko, D. V. 1987. Possible effects of pre-existing basement topography on thrust fault ramping. *J. Struct. Geol.* **9**, 1029–1039.

Seguret, M. & Daignières, M. 1986. Crustal scale balanced cross sections of the Pyrenees: discussion. In: *The Geological Evolution of the Pyrenees* (edited by Banda, E. & Wickham, S. M.). *Tectonophysics* **129**, 303–318.

Sibson, R. H., Francois, R. & Poulsen, K. H. 1988. High-angle reverse faults, fluid-pressure cycling, and mesothermal gold–quartz deposits. *Geology* **16**, 551–555.

Sibson, R. H., McM. Moore, K. & Rankin, A. H. 1975. Seismic

pumping—a hydrothermal fluid transport mechanism. *J. geol. Soc. Lond.* **131**, 653–659.
Teufel, C. W. 1980. Precursive pore pressure changes associated with premonitory slip during stick-slip sliding. *Tectonophysics* **69**, 189–199.
Teufel, C. W. 1981. Pore volume changes during frictional sliding of simulated faults. In: *Mechanical Deformation of Crustal Rocks. Am. Geophys. Un. Geophys. Monogr.*, 135–145.
Van Lith, J. G. J. 1965. Geology of the Spanish part of the Gavarnie Nappe (Pyrenees) and its underlying sediments near Bielsa (Province of Huesca). *Geologica Ultraiectina* **10**, 5–64.
Walder, J. & Nur, A. 1984. Porosity reduction and crustal pore pressure development. *J. geophys. Res.* **89**, 11,539–11,548.
Williams, G. D. & Fischer, M. W. 1984. A balanced cross-section across the Pyrenean orogenic belt. *Tectonics* **3**, 773–780.
Zwart, H. J. 1979. The geology of the Central Pyrenees. *Leidse Geol. Med.* **50**, 1–74.